

# PHYSICAL REVIEW LETTERS

---

---

VOLUME 78

3 MARCH 1997

NUMBER 9

---

---

## Theory of an Output Coupler for Bose-Einstein Condensed Atoms

R. J. Ballagh,<sup>1</sup> K. Burnett,<sup>2</sup> and T. F. Scott<sup>1</sup>

<sup>1</sup>*Department of Physics, University of Otago, P.O. Box 56, Dunedin, New Zealand*

<sup>2</sup>*Clarendon Laboratory, Department of Physics, University of Oxford, Parks Road, Oxford OX1 3PU, United Kingdom*  
(Received 1 November 1996)

The evolution of a two component Bose-Einstein condensate, consisting of atoms in two distinct hyperfine states, is modeled using a generalization of the Gross-Pitaevskii equation. Coherent coupling of the components by a microwave or RF field gives rise to a range of spatiotemporal behaviors, controlled by the strength and detuning of the applied field. From an initial trapped single component state, a second component can be generated which may escape from the trapping region or remain trapped within the first component. The initiating mechanism is identified and characterized. [S0031-9007(97)02539-8]

PACS numbers: 03.75.Fi, 05.30.Jp, 67.90.+z

Following the first observations of Bose-Einstein condensation in an atomic gas in 1995 [1,2] attention is now turning to exploring the properties of this new state of matter. A number of studies of the dynamical properties of the condensates have now been made at JILA and MIT [3,4]. These studies have confirmed the validity of the mean-field approaches to modeling atomic Bose-Einstein condensed gases around  $T \approx 0$ . Recently [5], the MIT group have demonstrated coherent transfer of an initially trapped condensate into another atomic state, which may escape the trap and form a coherent atomic beam. Such an output coupling mechanism may eventually constitute an important element of an atom laser, indeed some would claim that the experiment constitutes a realization of a pulsed atom laser.

In this Letter we present a theoretical study of an output coupler based on a closely related mechanism, namely coherent coupling between internal atomic states of the condensate. Zeng *et al.* [6] have also studied the coherent coupling of internal condensate states, but a key additional feature of the present paper is the inclusion of spatial effects. For simplicity we shall assume the atom has two states,  $|1\rangle$  and  $|2\rangle$ , with the initial condensation occurring in the trapped state  $|1\rangle$ . State  $|2\rangle$ , which has different trapping properties and is typically unconfined by the magnetic trap, is coupled to  $|1\rangle$  by an RF or microwave field tuned near the  $|1\rangle \rightarrow |2\rangle$  transition. The

interaction of the field may thus generate condensate in state  $|2\rangle$ , from an initial condensate which is entirely in state  $|1\rangle$ . In one of their experiments, the MIT group used a broad band short pulsed field to couple different Zeeman states. In others, they used a longer duration, nearer to monochromatic field to transfer condensate out of the trap [7]. Here, we shall examine the effects of a monochromatic field and show that it can lead to a variety of behaviors controlled by the amplitude and detuning of the coupling field. For example, the condensate in state  $|2\rangle$ , although untrapped by the magnetic potential, may become completely trapped within the first condensate by the mean field. In other situations, direct escape from the trapping region occurs. A rich set of phenomena arises from the interplay of the coherent coupling features with the other mechanisms characteristic of alkali atom condensates, predominantly the mean-field and the trapping potential. The coherent coupling gives rise to certain features that are familiar from the well known two-state Rabi behavior, but important new features with an essential spatial character arise, and these can be used to modify and control the spatial evolution of the interacting condensates. In this Letter we focus on novel aspects of this system which may also be of relevance in the eventual design of an atom laser.

We illustrate a specific realization of our scheme in Fig. 1 which is a level diagram of the  $F = 2$  and  $F = 1$

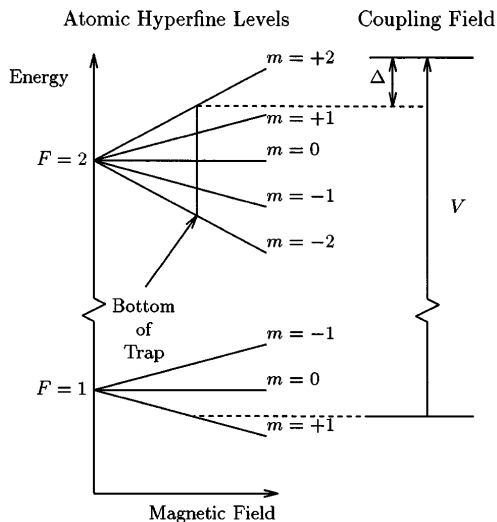


FIG. 1. Coherent coupling scheme between Rubidium ground level states.

hyperfine levels of the  $5S_{1/2}$  manifold of  $^{87}\text{Rb}$ . This diagram is appropriate to the experiment of Anderson *et al.* [1], where condensation was achieved in the  $|F=2, M=2\rangle$  state. A circularly polarized microwave field of  $\approx 7$  GHz will couple this trapped state to the anti-trapped  $|F=1, M=1\rangle$  state. Alternatively, an RF field within the  $F=2$  hyperfine manifold could be used to couple a trapped  $|F=2, M=1\rangle$  state to the untrapped  $|F=2, M=0\rangle$  state. We note that while we have taken the particular example of rubidium, a similar coupling scheme will apply to other alkali atoms.

The equations we use to describe this system are derived using a second quantized many body field theoretical treatment. The Hamiltonian is of similar form to the standard bosonic case for atoms undergoing binary elastic collisions [8], but generalized to account for the two internal atomic states  $|1\rangle$  and  $|2\rangle$ , coupled by magnetic dipole interaction with the oscillating magnetic field  $\mathbf{B}\cos(\omega\tau)$ . In state  $|1\rangle$  the atom experiences an attractive harmonic potential, while in state  $|2\rangle$  the potential is different by a factor of  $k$  which may be zero, or even negative (an anti-trapped state). Applying a mean-field approximation to the equations for the field operators, as in the derivation of the well known Gross-Pitaevskii equation [8], we obtain the following equation for the mean fields (or order parameters)  $\Psi_1(\mathbf{r}, \tau)$  and  $\Psi_2(\mathbf{r}, \tau)$  of the two states:

$$\begin{aligned} \frac{\partial \Psi_1}{\partial \tau} &= i\nabla^2 \Psi_1 - \frac{i}{4} r^2 \Psi_1 \\ &\quad - iC(|\Psi_1|^2 + 2|\Psi_2|^2)\Psi_1 + iV\Psi_2, \\ \frac{\partial \Psi_2}{\partial \tau} &= i\nabla^2 \Psi_2 - \frac{ik}{4} r^2 \Psi_2 \\ &\quad - iC(|\Psi_2|^2 + 2|\Psi_1|^2)\Psi_2 + iV\Psi_1 - i\Delta\Psi_2. \end{aligned} \quad (1)$$

Here  $\mathbf{r}$  and  $\tau$ , the spatial and temporal coordinates, are scaled in harmonic oscillator units (see, for example, Ref. [9]) and the nonlinearity parameter  $C$  is given by  $C = NU_0/\hbar\omega$  where  $N$  is the number of atoms and  $U_0$  is the  $s$ -wave scattering effective interaction strength (e.g., Ref. [9]), appropriately generalized to two components [10]. We can be confident of the validity of mean-field theory for these systems, given its success in predicting the excitation spectrum [11,12]. For simplicity we have assumed the scattering interaction is independent of the internal state of the atoms. Furthermore, we have ignored loss and growth mechanisms so that  $N$  is fixed. The coherent coupling is described by the terms  $iV\Psi_2$  and  $iV\Psi_1 - i\Delta\Psi_2$  in the above equations, where the parameter  $V = \mathbf{m} \cdot \mathbf{B}/\hbar$  is the bare Rabi frequency, (with  $\mathbf{m}$  the magnetic dipole between states  $|1\rangle$  and  $|2\rangle$ ) and  $\Delta$  is the detuning (see Fig. 1). The mean fields are normalized according to

$$\int_{-\infty}^{\infty} (|\Psi_1|^2 + |\Psi_2|^2) d^3r = 1. \quad (2)$$

In general, the coupled equations for  $\Psi_1$  and  $\Psi_2$  must be solved numerically. In this paper we limit ourselves to the one dimensional case so that in Eq. (1),  $\nabla^2 \rightarrow \partial^2/\partial x^2$  where  $x$  is the spatial variable, and we have obtained solutions over a wide variety of parameter regimes. Although as expected with coupled nonlinear partial differential equations, there are many variants of behavior, nevertheless some important physical trends emerge. Here we report and explain the most important of these and demonstrate some distinctive and perhaps unanticipated behavior that can arise from them. In all of the following cases, we have set  $k=0$  in Eq. (1) so that state  $|2\rangle$  is untrapped.

At large values of  $V$  or  $|\Delta|$ , a simple form of cycling between the two condensates occurs that is reminiscent of the Rabi cycling familiar from NMR or quantum optics. We illustrate this behavior in Fig. 2 for the case of  $V=35$  and  $\Delta=5$ , where we have chosen the initial state to be a trapped condensate eigenstate [13] with all atoms in internal state  $|1\rangle$ . For this case, each spatial part of the condensate has the same cycling period, and this is sufficiently short that the time spent in state  $|2\rangle$  is too brief to allow the untrapped condensate to escape. When the values of  $V$  and  $|\Delta|$  are small (compared to the chemical potential, see below) the cycling behavior may begin to exhibit distinct spatial character. This can be seen in Fig. 3 where  $V=2$  and  $\Delta=-5$ , and the initial condensate again begins in a trapped eigenstate. Over the time duration shown, the kinetic energy terms in Eq. (1) have little effect in mixing spatial locations, so that the shape of the condensates is determined largely by the cycling. The salient feature is that now the cycling varies spatially and it has a maximum modulation in a relatively narrow spatial range, causing the second condensate to form predominantly in this region.

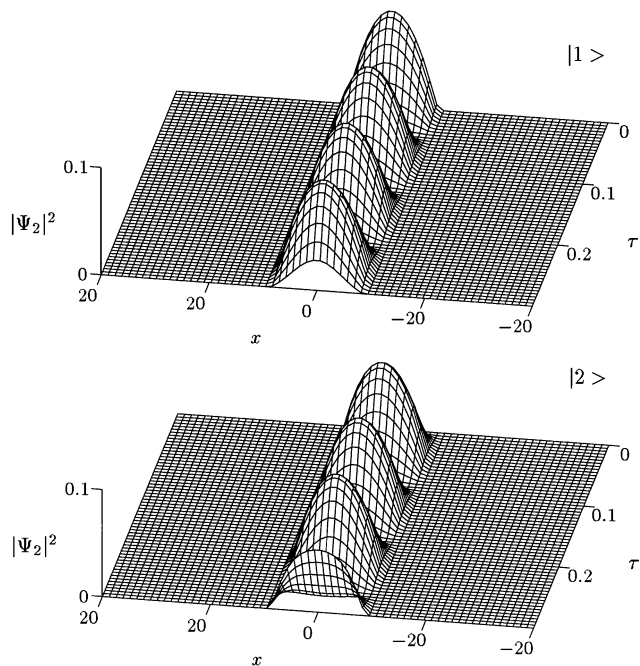


FIG. 2. Evolution of condensate density for each component, for the case  $C = 200$ ,  $V = 35$ , and  $\Delta = 5$ .

We can obtain an analytic understanding of this behavior by considering Eq. (1) in the Thomas-Fermi regime [14] and using the formal similarity of the equations to the classic Rabi problem, to give the following approxi-

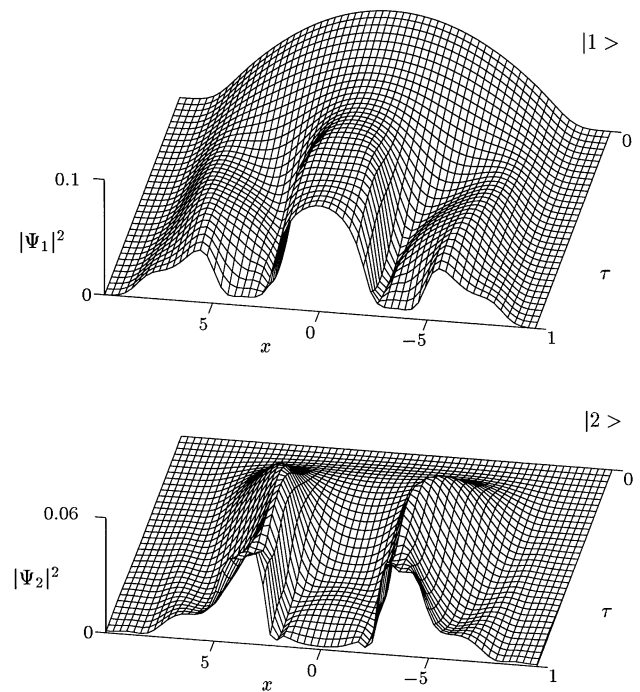


FIG. 3. Evolution of condensate density for the case  $C = 200$ ,  $V = 2$ , and  $\Delta = -5$ .

mate expression for the initial evolution of the density of component  $|2\rangle$ :

$$|\Psi_2(x, \tau)|^2 = |\Psi_1(x, 0)|^2 \frac{2V^2}{\Omega(x)^2} (1 - \cos[\Omega(x)\tau]). \quad (3)$$

In obtaining this equation we have neglected the factor of 2 in the exchange terms in Eq. (1), allowing us to approximate the self interaction terms by  $C|\Psi_1(x, \tau = 0)|^2$ . The spatially dependent cycling frequency  $\Omega(x)$  is given by

$$\Omega(x) = \sqrt{\Delta_{\text{eff}}^2 + 4V^2}, \quad (4)$$

where the effective detuning is

$$\Delta_{\text{eff}} = C|\Psi_1(x, 0)|^2 + \Delta - \frac{1}{4}x^2 \approx \mu + \Delta - \frac{1}{2}x^2. \quad (5)$$

The final form for  $\Delta_{\text{eff}}$  in Eq. (5) is obtained from the Thomas-Fermi form of the wave function  $|\Psi(x, \tau = 0)|^2 = (\mu - x^2/4)/C$ , where the chemical potential is given by  $\mu = (3C/8)^{2/3}$  and the wave function is considered zero except between  $-2\sqrt{\mu} < x < 2\sqrt{\mu}$ . Condensate  $|2\rangle$  reaches a peak on-axis density at  $\tau = \pi/\Omega(0)$ , and thus the condition for the cycling of the condensate to be independent of spatial location (i.e., as in Fig. 2) is that  $\Omega(x)/\Omega(0) \approx 1$  across the wave function, i.e.,

$$\Delta^2 + 4V^2 \gg \mu(\mu + 2|\Delta|). \quad (6)$$

When this latter condition is not met, spatial variation of the cycling may give rise to a more complex spatial shape with narrow maxima and minima of density, such as seen in Fig. 3. The initial spatial maximum in  $|\Psi_2(x)|^2$  arises largely from the variation of the factor  $|\Psi_1(x, \tau = 0)|^2 2V^2/\Omega(x)^2$  in Eq. (3) which peaks at  $x_p = \pm[4\mu - 2([\mu - \Delta]^2 + 4V^2)^{1/2}]^{1/2}$ . A useful simple estimate of  $x_p$  is obtained as being the position where  $\Delta_{\text{eff}}$  vanishes, i.e., at  $x_p \approx \pm\sqrt{2(\mu + \Delta)}$ , which will be real, and within the extent of the Thomas-Fermi wave function, provided  $-\mu < \Delta < 2\mu$ .

Once sufficiently sharp spatial features develop that the time scale for kinetic energy initiated spatial diffusion is comparable to the cycling time, the Thomas-Fermi treatment is no longer valid. Other mechanisms, in particular mutual repulsion of the two condensates, may now begin to play a significant role in the condensate evolution and cause dramatically different long time behavior as we now illustrate. In Fig. 4, where the parameters are the same as in Fig. 3, except here  $\Delta = +10$ , condensate  $|2\rangle$  is formed near the edges of condensate  $|1\rangle$ , and subsequently steadily escapes the trap. Condensate  $|1\rangle$  occupies the central region, and the coherent collisional repulsion between condensates (which is twice as large as the collisional self interaction) acts to push condensate  $|2\rangle$  away from the trap region. This configuration represents an output coupler, since condensate  $|2\rangle$  continually forms at the

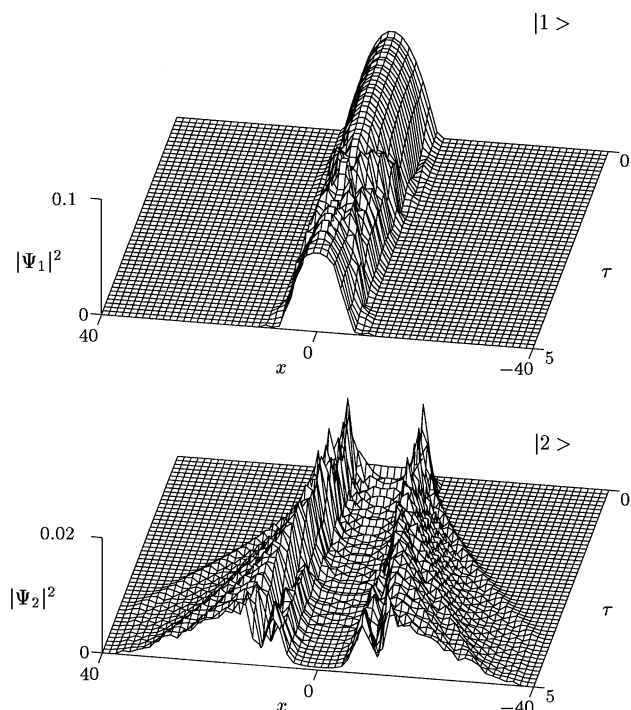


FIG. 4. Evolution of condensate density for the case  $C = 200$ ,  $V = 2$ , and  $\Delta = 10$ .

edges of condensate  $|1\rangle$ , and streams off as a coherent atomic beam.

In Fig. 5, by contrast, a situation is produced where the central region is occupied by condensate  $|2\rangle$  alone, and is surrounded by condensate  $|1\rangle$ , which itself is confined by the trapping potential. The mutual collisional repulsion compresses the nominally untrapped condensate  $|2\rangle$  and prevents its escape. This configuration is produced using exactly the same parameters as Fig. 3, but with the external field turned off after  $\tau = 1.2$ . The initial propagation is given in Fig. 3, but immediately following this cycling dominated regime, collisional repulsion and diffusion become the dominant mechanisms and combine to produce a very deep minimum in the center of condensate  $|1\rangle$ , which fills with condensate  $|2\rangle$ . Once the external field is turned off, mutual repulsion quickly expels vestiges of the minority condensate from either region, leading to the final configuration. Our simulations show this to be long lived and stable against spatial fluctuations. The stability mechanism is that condensate  $|2\rangle$  tends to expand by diffusion, while the trapping potential compresses condensate  $|1\rangle$  towards the center of the trap. Mutual repulsion prevents the condensates from merging together.

We have seen that a plane wave external field can generate a second condensate coherent with the first, and the spatial character of the *two* condensates may be manipulated by simply altering the strength or detuning of the external field. Although our simulations are carried out only in one spatial dimension, they may be

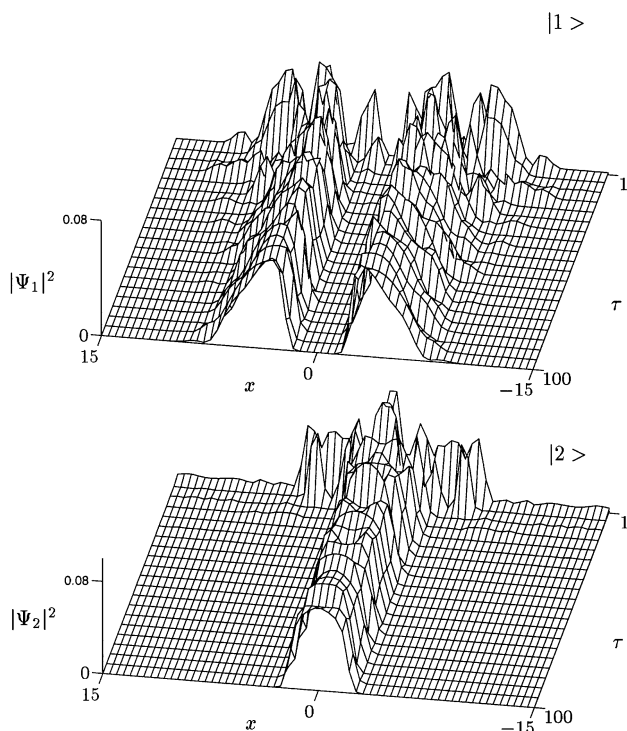


FIG. 5. Evolution of condensate density for the same parameters as in Fig. 3, but with the coupling field turned off at  $\tau = 1.2$ .

immediately applicable to the “cigar” shaped condensates that the MIT group is now producing with their cloverleaf trap [15]. Furthermore, we expect that many of the important properties we have discussed will carry over into fully three dimensional calculations. For the MIT sodium condensate, the value  $V = 35$  corresponds to a value of  $\mathbf{B} = 1.3$  mG,  $\Delta = 10$  corresponds to 1.1 kHz, and  $C = 200$  corresponds (in the 3D case, see Ref. [9]) to  $N \approx 65\,000$ .

Perhaps of most immediate interest is the possibility we have shown of using the external electromagnetic field to produce a controllable output coupler for atom fields. In three dimensions, it may prove feasible to combine a trap geometry for condensate  $|1\rangle$  with the choice of external field parameters in such a way that condensate  $|2\rangle$  forms near the edge, in one spatial dimension only. Thus it would be confined in two dimensions and escape in one dimension as a directed coherent matter beam.

This work was supported financially by the New Zealand Marsden Fund under Contract PVT 603. T.S. wishes to thank Dr. N. Mulgan for helpful discussions.

- 
- [1] M.H. Anderson, J.R. Ensher, M.R. Matthews, C.E. Wieman, and E. A. Cornell, *Science* **269**, 198 (1995).  
 [2] K.B. Davis, M.-O. Mewes, M.R. Andrews, N.J. van Druten, D.S. Durfee, D.M. Kurn, and W. Ketterle, *Phys. Rev. Lett.* **75**, 3969 (1995).

- 
- [3] D. S. Jin, J. R. Ensher, M. R. Matthews, C. E. Wiemann, and E. A. Cornell, *Phys. Rev. Lett.* **77**, 420–423 (1996).
- [4] M. O. Mewes, M. R. Andrews, N. J. van Druten, D. M. Kurn, D. S. Durfee, C. G. Townsend, and W. Ketterle, *Phys. Rev. Lett.* **77**, 988–991 (1996).
- [5] M. -O. Mewes, M. R. Andrews, D. M. Kurn, D. S. Durfee, C. G. Townsend, and W. Ketterle, *Phys. Rev. Lett.* (to be published).
- [6] Heping Zeng, Weiping Zhang, and Fucheng Lin, *Phys. Rev. A* **52**, 2155 (1995).
- [7] W. Ketterle (private communication).
- [8] E. M. Lifshitz, and L. P. Pitaevskii, *Statistical Physics* (Pergamon Press, Oxford, 1980), Pt. 2.
- [9] P. A. Ruprecht, M. J. Holland, K. Burnett, and M. Edwards, *Phys. Rev. A* **51**, 4704 (1995).
- [10] P. S. Julienne, A. M. Smith, and K. Burnett, in *Advances in Atomic, Molecular and Optical Physics*, edited by D. R. Bates and B. Bederson (Academic, San Diego, California, 1993).
- [11] S. Stringari, *Phys. Rev. Lett.* **77**, 2360 (1996).
- [12] M. Edwards, P. A. Ruprecht, K. Burnett, R. J. Dodd, and C. W. Clark, *Phys. Rev. Lett.* **77**, 1671 (1996).
- [13] M. Edwards, R. J. Dodd, C. W. Clark, P. A. Ruprecht, and K. Burnett, *Phys. Rev. A* **53**, R1950 (1996).
- [14] M. Edwards and K. Burnett, *Phys. Rev. A* **51**, 1382 (1995).
- [15] M. O. Mewes, M. R. Andrews, N. J. van Druten, D. M. Kurn, D. S. Durfee, and W. Ketterle, *Phys. Rev. Lett.* **77**, 416 (1996).